

## **Homotopy perturbation method for a limit case Stefan problem governed by fractional diffusion equation**

### **2.1 Introduction**

The mathematical model of the movement of the shoreline in a sedimentary ocean basin (A Shoreline Problem) is a generalized Stefan problem with variable latent heat. Swenson et al. (2000) utilized an analogy with one-phase melting problem and developed a mathematical model (fluvio- deltaic sedimentation model) for movement of shoreline in a sedimentary basin in response to changes in sediment line flux, tectonic subsidence of earth's crust and sea level change. Voller et al. (2004) presented an analytical similarity solution for a Stefan problem with variable latent heat which is a limit case of the above model. Later, Capart et al. (2007) presented mathematical solutions for several sedimentary problems featuring semi-infinite alluvial channels evolving under diffusional sediment transport. Voller et al. (2006) discussed a novel moving boundary problem related to shoreline movement in a sedimentary basin, which was solved by enthalpy method. In 2009, Rajeev et al. (2009) presented a numerical method for a moving boundary problem (Stefan problem) with variable latent heat and the comparisons were made with the results of Voller et al. (2004).

The classical diffusion transport models (Swenson (2000), Paola et al. (1992) and Pelletier et al. (1997)) provide a reliable means of modelling the sediment transport in fluvial depositional systems. The assumptions

of the classical diffusion equation are thin-tailed periods of inactivity and thin-tailed transport distances for sediment particles. In recent years, the fractional derivative operators are widely used for describing many real physical processes (Metzler (2000, 2004) and Kilbas et al. (2006)). Benson et al. (2001) pointed that non-integer calculus almost dates back to the initial developments of the integer calculus; care needs to be taken in defining and evaluating the fractional derivatives in transport equations. Some studies (Schumer et al. (2009), Ganti et al. (2009), Nathan Bradley et al. (2010) and Foufoula-Georgiou et al. (2010)) have observed the deviation from normal (Fickian) diffusion in sediment tracer dispersion that violates the assumption of statistical convergence to a Gaussian. Nikora et al. (2002) hypothesized that particle motion at short time scales is super diffusive because of inertia, while long-time sub diffusion results from heavy-tailed rest durations between particle motions. It is observed by Schumer et al. (2003) and Meerschaert et al. (2004) that a pure power-law, heavy-tailed probability density function for the periods of inactivity without any truncation leads to a time-fractional diffusion equation which describes the evolution of surface elevation in time. Voller and Paola (2010) presented the deviation of fluvial profiles from ones predicted by classical diffusion and proposed the exploration of fractional diffusive model to describe the observed steady-state fluvial profiles in a depositional system. Ganti et al. (2011) discussed time fractional diffusion model for the surface dynamics of depositional systems by considering the fact that the periods of inactivity are heavy-tailed. They also discussed physical mechanisms constrain for the occurrence of extremes in depositional systems and how these constraints reflect in the probability distributions of the random variables. They also presented that preliminary thoughts on continuum models for surface evolution of depositional systems are consistent with

the documented probability distributions for erosional, depositional and inactivity events. These models motivate to discuss fractional diffusion model in sedimentation process to study the physical effect in complex domain. Recently, Martin et al. (2012) discussed the physical basis for anomalous diffusion in bed load transport.

Exact solutions to the Stefan problem with anomalous diffusion are discussed by Liu and Xu (2004), Junyi and Xu (2009) and Li et al. (2007, 2008). Voller (2010) also presented an exact solution of a limit case Stefan problem governed by a fractional diffusion equation and discussed the utility of fractional derivative in diffusion process. The Stefan problem is a special nonlinear problem which is difficult to get the exact solution (Crank (1987), Carslaw and Jaeger (1987)). Therefore, many approximate methods have been used to solve the Stefan problem, e.g., the perturbation method (Lin and Ping (2005)), combination of variable method (Abdekhodaie and Cheng (1996)), variational iteration method and Adomian decomposition method (Das and Rajeev (2010)), etc. The approximate analytical approach taken in this literature is homotopy perturbation method. Homotopy perturbation method was first proposed by He (1999, 2000, 2003, 2004) and successfully applied to solve various nonlinear problem (He (2004, 2005)). Li et al. (2009) successfully extended homotopy perturbation method to solve time-fractional diffusion equation with a moving boundary condition. Recently, some researchers (Das et al.(2011), Rajeev (2014), Singh et al.(2011)) also used this technique to solve moving boundary problems.

In present study, we consider the non-classical or non-Fickian, anomalous sediment transport in braided networks, which are known to have fractal planform geometry. Anomalous diffusion process occurs when the variance of the transported quantity grows in time as  $t^\alpha$ . The case with  $0 < \alpha < 1$  is known as the sub diffusion regime,  $\alpha = 1$  corresponds to the normal diffusion, and  $\alpha > 1$  is

known as the super diffusion regime. Our attention in this chapter will be focused on the time-fractional diffusion equations of a single or distributed order less than 1, which are known to be models for sub-diffusive processes. The main physical purpose for adopting and investigating diffusion equations with fractional time derivative is to describe phenomena of anomalous (non-Fickian) sediment transport through complex and/or disordered systems including fractal media which occurs in sedimentation process. A pure power-law, heavy-tailed probability density function for the periods of inactivity without any truncation is taken into account. An approximate analytical solution by homotopy perturbation method for a limit case of Stefan problem with variable latent heat governed by fractional derivative in Caputo sense is also presented. The obtained results are compared with the existing exact solutions. A brief sensitivity study is also performed.

## 2.2 The Shoreline model

Shoreline problem involves the shoreline propagation in a sedimentary ocean basin due to a sediment line flux, tectonic subsidence of the earth's crust, and sea level change. The governing differential equations for the sediment transport and deposition in a sub-aerial, fluvial domain (a net depositional river basin) is given by the following diffusion equation (Swenson et al. (2000), Voller et al. (2004)):

$$\frac{\partial \eta}{\partial t} = \nu \frac{\partial^2 \eta}{\partial x^2} + \frac{\partial h}{\partial t}, \quad 0 \leq x \leq s(t), \quad (2.2.1)$$

where  $\eta(s, t)$  is the height of the sediment above a datum,  $\nu$  is the effective fluvial diffusivity, which depends primarily on the water discharge in the river system, and  $h$  is height of earth's crust. The boundary conditions on (2.2.1) are:

$$\nu \frac{\partial \eta}{\partial x} \Big|_{x=0} = -q(t) \quad \text{and} \quad \eta(s, t) = z(t), \quad (2.2.2)$$

where  $q$  is prescribed sediment line flux and  $z(t)$  is ocean level above the datum.

A condition for the advance or retreat of the shoreline in an offshore submarine domain (Swenson et al. (2000), Voller et al. (2004)) is given by:

$$-v \frac{\partial \eta}{\partial x} \Big|_{s(t)} = (u - s) \left[ a \frac{ds}{dt} + \frac{dz}{dt} \right] - \int_s^u \frac{\partial h}{\partial t} dx, \quad (2.2.3)$$

with the initial condition  $s(0) = 0$ . (2.2.4)

where  $a$  is slope of the offshore sediment wedge and  $u(t)$  is the lateral position where the toe of the submarine sediment wedge intersects the ocean basement. A schematic cross section of such a basin indicating the variables is shown in Fig. 2.1 (Voller et al., 2004).

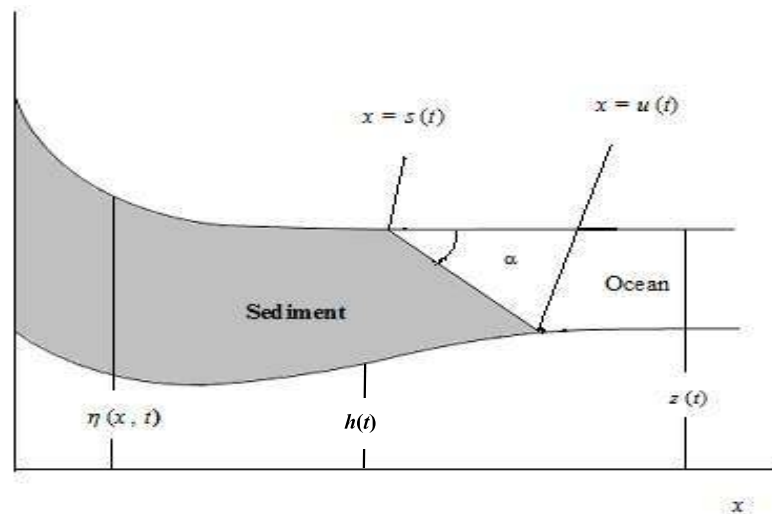


Fig. 2.1 A schematic cross section of sedimentary ocean basin

### 2.3 Mathematical formulation for a limit case

In this section, a fractional model of a limit case for shoreline problem is presented. The model involves a shoreline problem with a fixed line flux, a constant ocean level ( $z = 0$ ), no tectonic subsidence of the earth's crust, and a constant sloping basement  $b < a$ . This scenario is a reasonable approximation for some modern continental margins. A geometrical construction of such a basin can be seen in the paper of Voller et al. (2004). Anomalous behavior (non-Fickian or non-classical) of sediment transport in heterogeneous domain is assumed. Moreover, a pure power-law, heavy-tailed probability density function for the periods of inactivity without any truncation is taken into account which leads to a time-fractional diffusion equation for describing the evolution of the height of the earth's crust (basement) above datum.

Under these limit cases the dynamics of the sedimentation process become Stefan problem with variable latent heat and the mathematical model is governed by time-fractional diffusion equation as described follows:

$$D_t^\alpha \eta(x,t) = v \frac{\partial^2}{\partial x^2} \eta(x,t), \quad (0 < x < s(t), \quad 0 < \alpha \leq 1), \quad (2.3.5)$$

with the following posed conditions:

$$v \left. \frac{\partial \eta}{\partial x} \right|_{x=0} = -q(t), \quad (2.3.6)$$

$$\text{and } \eta(s, t) = 0. \quad (2.3.7)$$

The additional conditions on the moving interface are

$$-v \left. \frac{\partial \eta}{\partial x} \right|_{x=s(t)} = \gamma s D_t^\alpha s(t), \quad (2.3.8)$$

$$\text{and } s(0) = 0, \quad (2.3.9)$$

where  $a(u-s) \frac{abs}{a-b} = \gamma s$  which is function of space and  $\gamma$  is a constant.

## 2.4 Solution of the problem by Homotopy Perturbation Method

According to the homotopy perturbation method (He (2003, 2005)), we construct the following simple homotopy for equation (2.3.5):

$$(1-p)v\frac{\partial^2\eta}{\partial x^2} + p\left[v\frac{\partial^2\eta}{\partial x^2} - D_t^\alpha \eta\right] = 0, \quad (2.4.10)$$

or

$$v\frac{\partial^2\eta}{\partial x^2} - p D_t^\alpha \eta = 0, \quad (2.4.11)$$

where  $p \in [0,1]$  is an embedding parameter. When  $p = 0$ , Eq. (2.4.11) becomes  $\frac{\partial^2\eta}{\partial x^2} = 0$ , which is easy to solve; and if  $p = 1$ , Eq. (2.4.11) turns out to be the equation Eq. (2.3.5). Assuming the following power series in  $p$  as the solutions of Eqs. (2.4.11) and (2.3.8):

$$\eta = \sum_{n=0}^{\infty} p^n \eta_n, \quad s = \sum_{n=0}^{\infty} p^n s_n. \quad (2.4.12)$$

The approximate solution of equation (2.3.5) can be obtained by setting  $p = 1$ , i.e.

$$\eta = \sum_{n=0}^{\infty} \eta_n, \quad s = \sum_{n=0}^{\infty} s_n. \quad (2.4.13)$$

Substituting (2.4.12) into (2.4.11), we obtain

$$\sum_{n=0}^{\infty} p^n v \frac{\partial^2}{\partial x^2} \eta_n = \sum_{n=0}^{\infty} p^{n+1} \frac{\partial^\alpha}{\partial t^\alpha} \eta_n. \quad (2.4.14)$$

Accordingly, the boundary condition (2.3.7) becomes

$$\sum_{m=0}^{\infty} p^m \eta_m \left( \sum_{n=0}^{\infty} p^n s_n, t \right) = 0. \quad (2.4.15)$$

As given by Li et al. (2009), the perturbation parameter  $p$  is both explicit and implicit parameter and the implicit part relates to the variable  $s$ . The explicit

form of  $p$  is needed to compare the coefficients of various powers of  $p$ . So, writing Taylor's series of  $\eta_i$  about a point  $(s_0, t)$  as:

$$\eta_i(x, t) = \sum_{n=0}^{\infty} \frac{1}{n!} \frac{\partial^n \eta_i}{\partial x^n} \Big|_{(s_0, t)} (x - s_0)^n, \quad i = 0, 1, 2, \dots$$

As a result, Eq. (2.4.15) becomes

$$\sum_{l=0}^{\infty} \sum_{m=0}^{\infty} \frac{p^l}{m!} \left( \sum_{n=1}^{\infty} p^n s_n \right)^m \frac{\partial^m}{\partial x^m} \eta_l(s_0, t) = 0, \quad (2.4.16)$$

and the interface condition (1.3.8) becomes

$$\sum_{l=0}^{\infty} \sum_{m=0}^{\infty} \frac{p^l}{m!} \left( \sum_{n=1}^{\infty} p^n s_n \right)^m \frac{\partial^{m+1}}{\partial x^{m+1}} \eta_l(s_0, t) = -\frac{\gamma}{\nu} \sum_{m=0}^{\infty} p^m s_m \left( \sum_{n=0}^{\infty} p^n D_t^\alpha s_n \right), \quad (x = s_0). \quad (2.4.17)$$

Comparing the terms with identical powers of  $p$  in (2.4.14), (2.4.16), (2.4.17), the following series of equations can be obtained:

$$\begin{aligned} p^0: \quad & \frac{\partial^2 \eta_0}{\partial x^2} = 0, \\ & \frac{\partial \eta_0(0, t)}{\partial x} \Big|_{x=0} = -\frac{q}{\nu}, \\ & \eta_0(s_0, t) = 0, \\ & \frac{\partial \eta_0(s_0, t)}{\partial x} = -\frac{\gamma}{\nu} s_0 D_t^\alpha s_0, \\ & s_0(0) = 0; \end{aligned} \quad (2.4.18)$$

$$\begin{aligned} p^1: \quad & \nu \frac{\partial^2 \eta_1}{\partial x^2} = D_t^\alpha \eta_0, \\ & \frac{\partial \eta_1(0, t)}{\partial x} = 0, \\ & \eta_1(s_0, t) + s_1 \frac{\partial \eta_0(s_0, t)}{\partial x} = 0, \end{aligned} \quad (2.4.19)$$

$$\frac{\partial \eta_1(s_0, t)}{\partial x} + s_1 \frac{\partial^2 \eta_0(s_0, t)}{\partial x^2} = -\frac{\gamma}{\nu} (s_0 D_t^\alpha s_1 + s_1 D_t^\alpha s_0),$$

$$s_1(0) = 0 ;$$

⋮

and so on.

Considering the first three equations of (2.4.18), we have

$$\eta_0 = \frac{q}{\nu} (s_0 - x). \quad (2.4.20)$$

Substituting it into fourth equation of (2.4.18), we get

$$s_0 = a_0 t^{\frac{\alpha}{2}}, \quad (2.4.21)$$

$$\text{where } a_0 = \sqrt{\frac{q}{\gamma}} \left[ \frac{\Gamma(1 - \frac{\alpha}{2})}{\Gamma(1 + \frac{\alpha}{2})} \right]^{1/2}.$$

Substituting  $s_0$  into (2.4.20), we get

$$\eta_0 = a_1 (a_0 t^{\alpha/2} - x), \quad (2.4.22)$$

where  $a_1 = q / \nu$ .

Substituting  $\eta_0$  and  $s_0$  into equation (2.4.19) and using the above process, we can obtain the following expressions of  $\eta_1$  and  $s_1$ :

$$\eta_1 = \frac{a_2 x^2}{2} t^{-\alpha/2} + (a_1 a_3 - \frac{a_2 a_0^2}{2}) t^{\alpha/2}, \quad (2.4.23)$$

$$s_1 = a_3 t^{\frac{\alpha}{2}}, \quad (2.4.24)$$

$$\text{where } a_2 = \frac{a_0 a_1}{v} \left[ \frac{\Gamma(1 + \frac{\alpha}{2})}{\Gamma(1 - \frac{\alpha}{2})} \right] \text{ and } a_3 = \frac{-a_2 v}{2\gamma} \left[ \frac{\Gamma(1 - \frac{\alpha}{2})}{\Gamma(1 + \frac{\alpha}{2})} \right].$$

Sequentially,  $\eta_2, s_2; \eta_3, s_3; \dots$  can be obtained.

Substituting  $\eta_0, s_0, \eta_1$  and  $s_1$  into the equation (2.4.13), the first order approximate solution can be obtained as:

$$\eta = a_1 \left( a_0 t^{\alpha/2} - x \right) + \frac{a_2 x^2}{2} t^{-\alpha/2} + \left( a_1 a_3 - \frac{a_2 a_0^2}{2} \right) t^{\alpha/2} \quad (2.4.25)$$

$$s = (a_0 + a_3) t^{\alpha/2} \quad (2.4.26)$$

which give height of the sediment above the datum and the shoreline position at a particular time.

## 2.5 Numerical comparison and discussion

In this section, numerical results for height of sediment  $\eta(x, t)$  and shoreline position  $s(t)$  are calculated for the fixed value of slope of basement ( $b = 1.5$ ) and slope of off-shore sediment wedge ( $a = 1.7$ ). The results are carried out using MATHEMATICA software and depicted through figures. All the calculations have been done by taking only two terms of the series for  $\eta(x, t)$  and  $s(t)$ . In order to compare the proposed approximate solution with the existing exact solution, we consider the following cases:

**Case1:** If  $\alpha = 1.0$  (standard motion) then it can be seen that

$$\eta = \frac{2q}{v} \left[ \lambda \left( \frac{e^{\frac{-x^2}{4tv}} + \pi^{\frac{1}{2}} v^{\frac{-1}{2}} \frac{x}{2\sqrt{t}} \operatorname{erf}\left(\frac{x}{2\sqrt{t}\sqrt{v}}\right)}{e^{\frac{-\lambda^2}{v}} + \pi^{\frac{1}{2}} v^{\frac{-1}{2}} \lambda \operatorname{erf}\left(\lambda v^{\frac{-1}{2}}\right)} \right) - \frac{x}{2\sqrt{t}} \right] \sqrt{t}, \quad (2.5.27)$$

$$s = 2\lambda\sqrt{t}, \quad (2.5.28)$$

where  $\lambda$  is the root of the following non-linear equation:

$$\frac{\pi^{\frac{1}{2}} v^{-\frac{1}{2}} \operatorname{erf}\left(\lambda v^{\frac{1}{2}}\right)}{e^{-\frac{\lambda^2}{v}} + \pi^{\frac{1}{2}} v^{-\frac{1}{2}} \lambda \operatorname{erf}\left(\lambda v^{\frac{1}{2}}\right)} - \frac{1}{\lambda} + \frac{2\gamma\lambda}{q} = 0, \quad (2.5.29)$$

are exact solutions to (2.3.5-2.3.9) as given in Voller et al. (2004).

Fig. 2.2 and Fig. 2.3 represent the dependence of height of sediment  $\eta(x,t)$  on space  $x$  for  $\alpha=1.0$  at fixed value of sediment line flux ( $q=0.5$ ) and time ( $t=2.5$  hours). It is seen from figures that the approximate solution is close to the exact solution for standard motion. Fig. 2.4 and Fig. 2.5 depict the accuracy of movement of shoreline position for integer order at a fixed value of sediment line flux ( $q=0.5$ ).

**Case 2:** For the comparisons of non standard motion ( $0 < \alpha < 1$ ), we consider the following Stefan problem that represents the process of solidification of a liquid in dimensionless form:

$$\frac{\partial^\alpha \eta(x,t)}{\partial t^\alpha} = \frac{1}{v} \frac{\partial^2 \eta(x,t)}{\partial x^2}, \quad (2.5.30)$$

$$\eta(0,t) = 0, \quad (2.5.31)$$

$$\eta(s(t),t) = 1, \quad (2.5.32)$$

$$\frac{\partial^\alpha s(t)}{\partial t^\alpha} = \frac{\partial \eta(s(t),t)}{\partial x}, \quad (2.5.33)$$

$$s(0) = 0. \quad (2.5.34)$$

Approximate solutions by homotopy perturbation method to (2.5.30) – (2.5.34) are given by:

$$\eta(x,t) = xa_0^{-1}t^{-\alpha/2} + a_1t^{-3\alpha/2}\frac{x^3}{3!} - \left(\frac{a_1a_0^2}{3!} + a_2a_0^{-2}\right)xt^{-\alpha/2}, \quad (2.5.35)$$

$$s(t) = (a_0 + a_2)t^{\alpha/2}, \quad (2.5.36)$$

where  $a_0 = \left(\frac{\Gamma(1-\frac{\alpha}{2})}{\Gamma(1+\frac{\alpha}{2})}\right)^{\frac{1}{2}},$

$$a_1 = va_0^{-1}\frac{\Gamma(1-\frac{\alpha}{2})}{\Gamma(1-\frac{3\alpha}{2})},$$

and  $a_2 = \frac{a_1a_0^2}{3}\left(\frac{\Gamma(1+\frac{\alpha}{2})}{\Gamma(1-\frac{\alpha}{2})} + a_0^{-2}\right)^{-1}.$

According to Junyi and Xu (2009), the exact solutions to (2.5.30 – 2.5.34) are

$$\eta(x,t) = \frac{1 - W\left(-x\sqrt{v}t^{-\frac{\alpha}{2}}; -\frac{\alpha}{2}, 1\right)}{1 - W\left(-p; -\frac{\alpha}{2}, 1\right)}, \quad (2.5.37)$$

and  $s(t) = \frac{p}{\sqrt{v}}t^{\frac{\alpha}{2}}, \quad (2.5.38)$

where  $W(-x, -\rho, 1 - \rho) = \sum_{n=0}^{\infty} \frac{(-x)^n}{n! \Gamma[-n\rho + (1 - \rho)]}$  is wright function and  $p$  is a constant

that will be determined by the following transcendental equation:

$$\frac{\Gamma(1+\frac{\alpha}{2})}{\Gamma(1-\frac{\alpha}{2})} p \frac{[1-W(-p;-\frac{\alpha}{2},1)]}{W(-p;-\frac{\alpha}{2},1-\frac{\alpha}{2})} = v. \quad (2.5.39)$$

Figs. (2.6–2.9) represent the comparison between exact result and approximate solution by homotopy perturbation method for different Brownian motion ( $\alpha = \frac{8}{9}, \frac{6}{7}, \frac{4}{5}, \frac{2}{3}$ ) at a fixed value of  $v = 1.0$ . It is seen from the figures that the error between proposed solutions and exact result increases with the decrease of the  $\alpha$  and/or the increase of time. But, the trends of graphs are similar. The authors are unable to find the reason for the increment in error as the value of  $\alpha$  decreases.

Fig. 2.10 and Fig. 2.11 represent the dependence of shoreline position on time for different Brownian motion  $\alpha = \frac{1}{3}, \frac{1}{2}, \frac{2}{3}$ , and also for the standard motion ( $\alpha = 1.0$ ) at  $q = 0.5$  and  $q = 1.0$ , respectively. It is observed from figures (2.10-2.11) that the rate of increase of  $s(t)$  decreases with the increase of  $\alpha$  which confirms the exponential decay of regular Brownian motion. This result is in good agreement with the result of Das and Rajeev (2010). It is also seen from Fig.2.10 and Fig.2.11 that for fixed values of  $a = 1.7, b = 1.5$ , if the sediment line flux  $q$  increases ( $q = 0.5, 1.0$ ), the movement of the shoreline position increases towards sea side with formation of inclined strata along the off-shore sediment wedge which confirms the result of Rajeev et al. (2009).

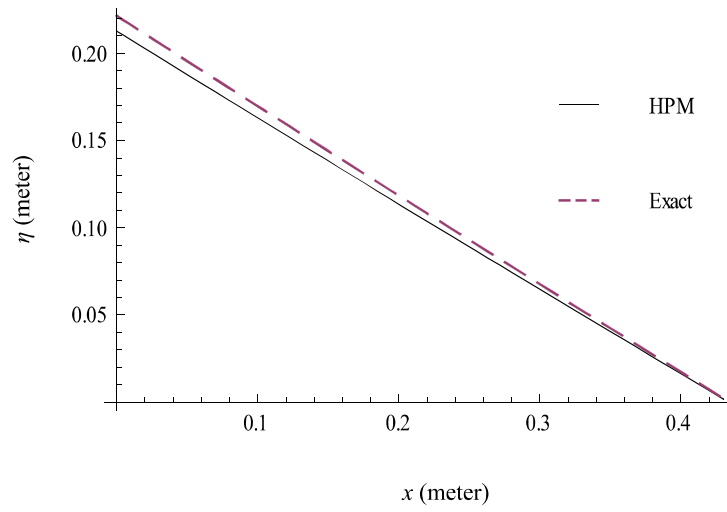


**Fig.2.2. Plot of  $\eta(x,t)$  vs.  $x$  for  $\nu=1.0$**

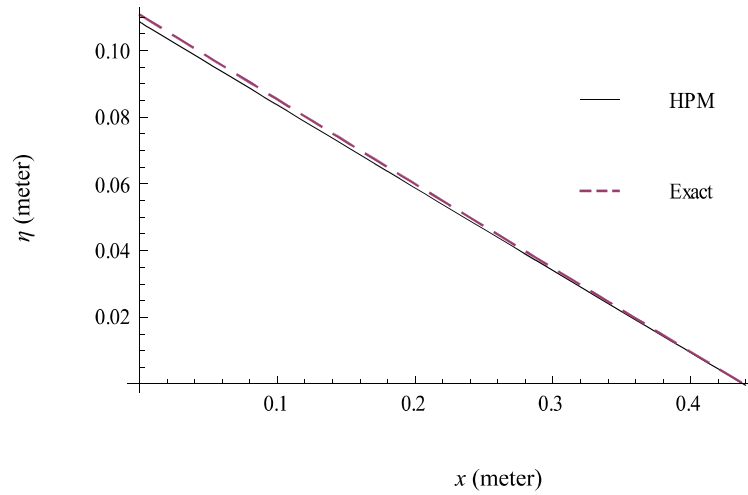


**Fig.2.3. Plot of  $\eta(x,t)$  vs.  $x$  for  $\nu=2.0$**

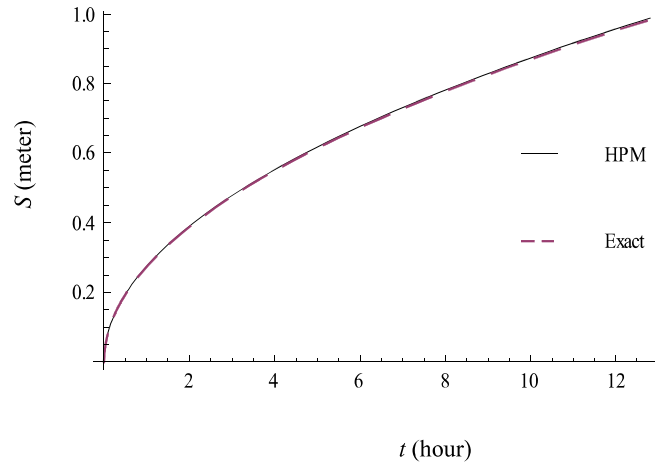


**Fig.2.4. Plot of  $s(t)$  vs.  $t$  for  $\nu = 1.0$**

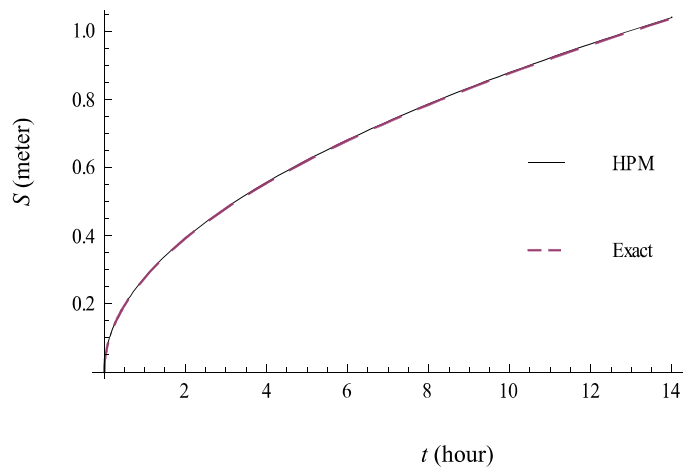


**Fig.2.5. Plot of  $s(t)$  vs.  $t$  for  $\nu = 2.0$**

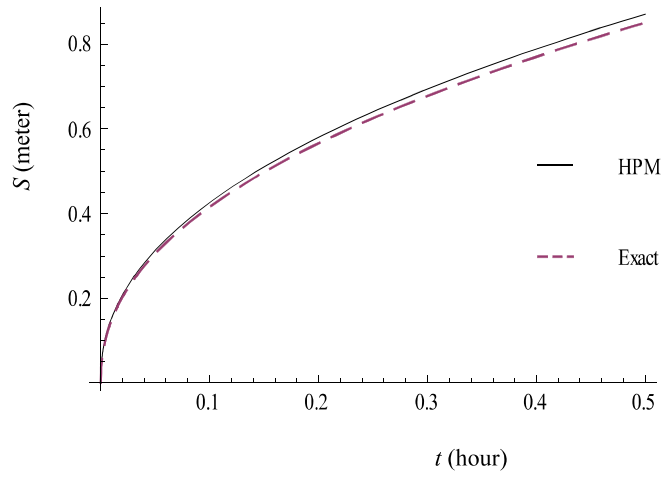


**Fig.2.6. Plot of  $s(t)$  vs.  $t$  at  $\nu=1.0$  for  $\alpha = 8 / 9$**

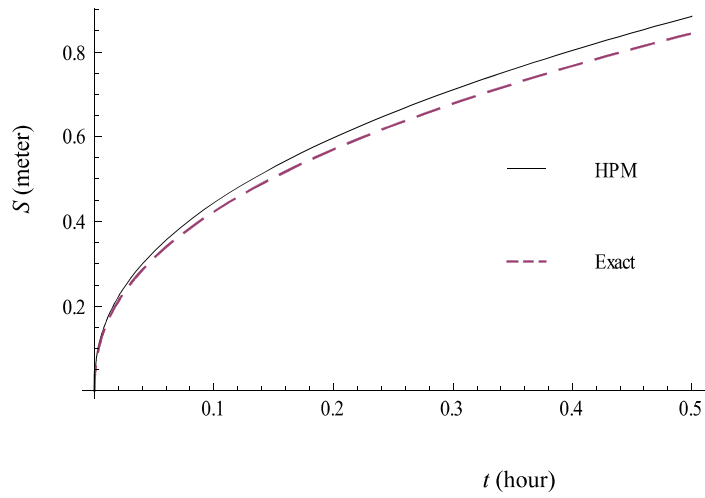


**Fig.2.7. Plot of  $s(t)$  vs.  $t$  at  $\nu=1.0$  for  $\alpha = 6/7$**

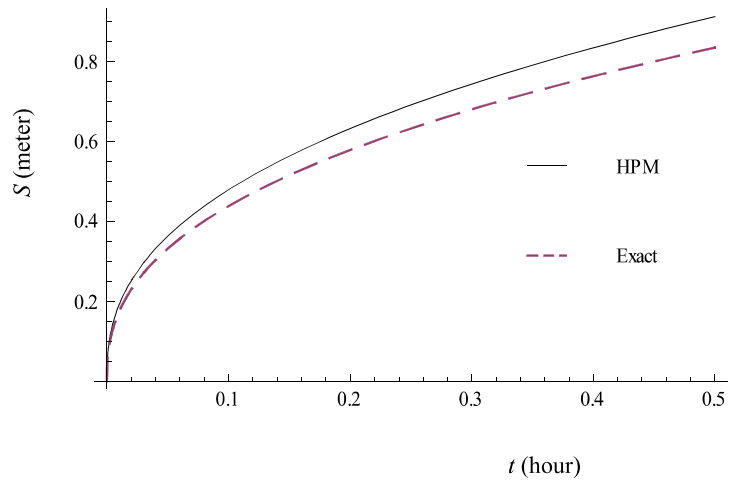


**Fig. 2.8.** Plot of  $s(t)$  vs.  $t$  at  $\nu=1.0$  for  $\alpha = 4/5$

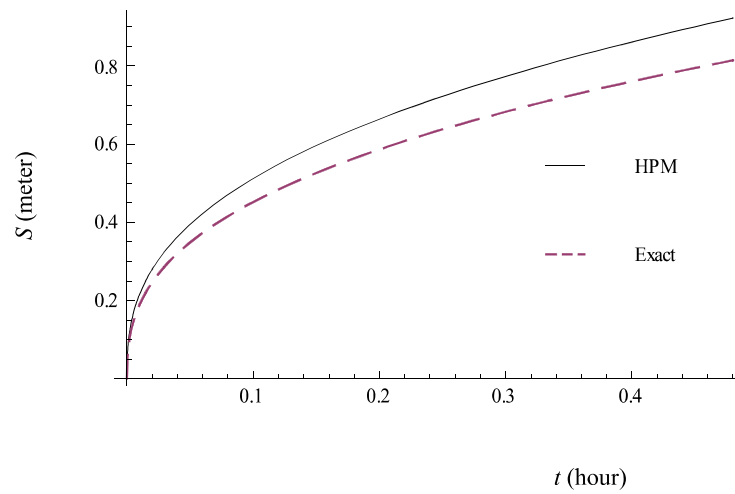


**Fig. 2.9.** Plot of  $s(t)$  vs.  $t$  at  $\nu=1.0$  for  $\alpha = 2/3$

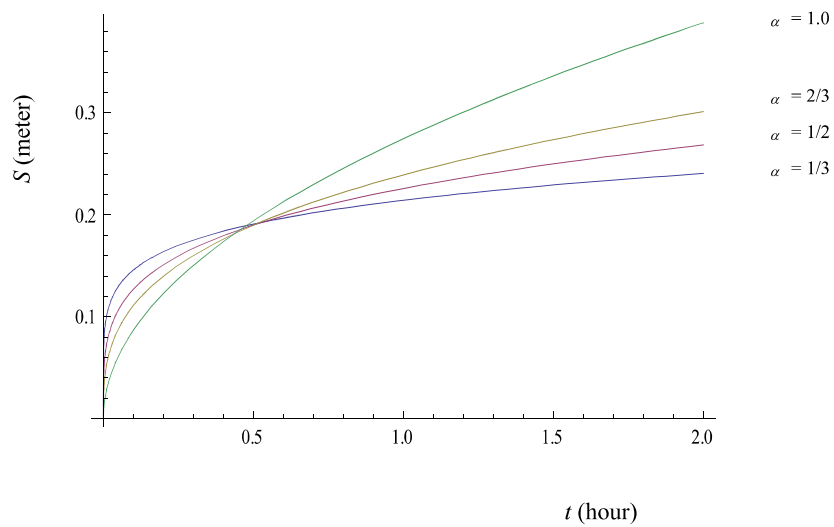


**Fig. 2.10. Plot of  $s(t)$  vs.  $t$  for  $q = 0.5$  and  $v = 1.0$**

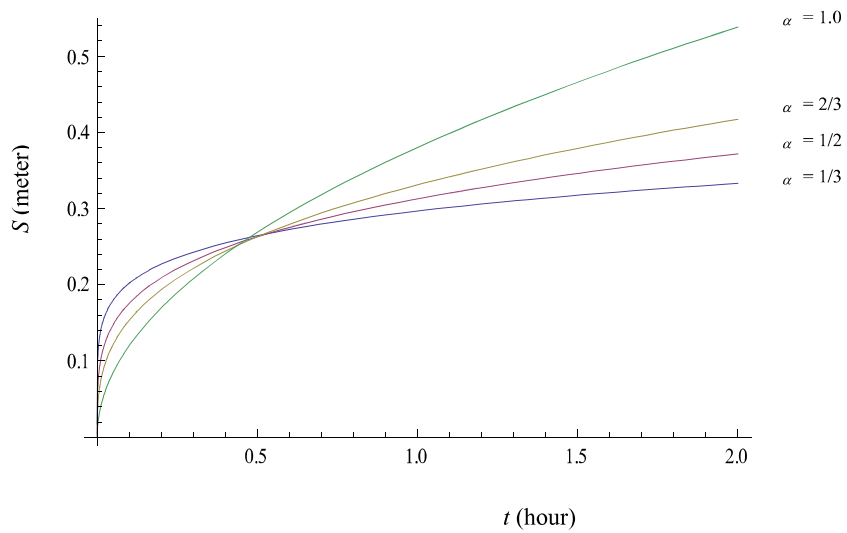


**Fig. 2.11. Plot of  $s(t)$  vs.  $t$  for  $q = 1.0$  and  $v = 1.0$**

## 2.6 Conclusion

In this work, we used the fractional derivative in Caputo sense and a model for a limit case of Stefan problem with variable latent heat governed by fractional derivative is presented. The solution of the proposed problem is obtained by homotopy perturbation method. The homotopy perturbation method is an efficient technique for solving various scientific and engineering problems. It is seen that homotopy perturbation method is a powerful and accurate method for finding the solution of Stefan problem for integer order. Moreover, it is straight forward and avoids the hectic work of calculations. Every method has its advantages and disadvantages. In present study, it is found that the proposed solutions by homotopy perturbation method deviate more from the exact solution with the decrease of the  $\alpha$  and/or the increase of time. It is also possible that this method may not be applicable at large times. However, the natures of graphs are similar. The authors believe that the procedure as described in the present study will be applicable to linear and nonlinear Stefan problems and it will considerably benefit to engineers and scientists working in this field.